Preparation of emulsions with a narrow particle size distribution using microporous α-alumina membranes

Goran T. Vladisavljević[a], Helmar Schubert[b]

[a]Institute of Food Technology and Biochemistry, Faculty of Agriculture, University of Belgrade, P.O. Box 127, YU-11081 Belgrade-Zemun, Serbia, Serbia and Montenegro. e-mail address: gtvladis@afrodita.rcub.bg.ac.yu

[b]Institute of Food Process Engineering, Faculty of Chemical Engineering, University of Karlsruhe (T.H.), Kaiserstrasse 12, D-76128 Karlsruhe, Germany. e-mail address: helmar.schubert@lvt.uni-karlsruhe.de

Contact author: G.T. Vladisavljević.

ABSTRACT

O/W emulsions with the smallest spans of particle size distribution (span = $(d_{90}-d_{10})/d_{50}$) reported till now for ceramic α-alumina membranes (0.42-0.56) were prepared using a 1.4-μm membrane cleaned thoroughly after use in an ultrasonic bath. The smallest span values of 0.42-0.48 were achieved at the transmembrane pressures 2.6-3.5 times greater than the capillary pressure. A narrow particle size distribution with the span of 0.48-0.49 was even obtained at the wall shear stress of 0.55 Pa, provided that the dispersed phase flux was not above 4.6 l m^2 h^{-1}. The span and mean droplet size were remarkably constant over the range of dispersed phase content of 1-10 vol. %. The membrane

cleaning by ultrasonication was one of the critical conditions for a successful operation. If the membrane was cleaned only by the cleaning in place (CIP) method the emulsions with a span value in the range of 0.7-1.4 were obtained.

INTRODUCTION

Membrane emulsification (ME) is a simple method developed by Nakashima et al. (1) for preparing monodispersed emulsions with the mean droplet size ranging from less than 1 μm to several tens of μm. In a ME system, dispersed phase is permeated through the membrane pores into a moving continuous phase under the driving force of transmembrane pressure differential (Fig. 1). The droplets are formed at the end of the pores at the membrane/continuous phase interface and carried away by the recirculating flow or stirring. The resulting particle size distribution (PSD) is primarily dictated by the membrane properties (surface wettability, mean pore size and pore size distribution), but it can be finely adjusted by the magnitude of process flow parameters, such as shear stress at the membrane surface and transmembrane pressure (2). Until now, the best ME results with regard to PSD were obtained using microporous glass membranes, such as a Shirasu porous glass (SPG) membrane developed by Nakashima and Shimizu (3). If the SPG membrane is not wetted with the dispersed phase and if process conditions and a surfactant type are properly chosen, the span of PSD of 0.26-0.45 can be typically obtained in the preparation of both W/O and O/W emulsions (4-9). The span of PSD is given by an equation: span = $(d_{90}-d_{10})/d_{50}$, where d_{x0} is the diameter corresponding to x0 vol. % on a relative cumulative PSD curve.

One of the disadvantages of SPG emulsification is a low dispersed phase flux, due to thick membrane wall and a small proportion of active pores. The direct microscopic observations of the SPG emulsification process revealed that only 0.3-0.5 % of the pores were simultaneously active at the dispersed phase flux of 2.8-28 l m^{-2} h^{-1} (10). In order to increase the production rate, some improvements of the conventional ME process were proposed, such as premix ME in which a pre-emulsion is pressed through the membrane instead of pure dispersed phase (11). However, a broader PSD was obtained with the span in the range of 0.4-0.65. Another possibility of increasing membrane productivity is the use of asymmetric porous glass membrane recently developed by Kukizaki et al. (12). The new applications of SPG technology in the synthesis of monodispersed microspheres and the preparation of drug delivery systems and food emulsions are reviewed by Nakashima et al. (13).

Apart from microporous glass membranes, other porous membranes were also used in ME, such as a microengineered silicon membrane (14), polymeric membranes (15-17), and ceramic α-alumina or zirconia membranes (18-21). Due to high dispersed phase flux and the resulting droplet-droplet interactions before detachment, polydispersed emulsions were obtained with a microengineered silicon membrane, although the pores were highly uniform (14). It shows that to obtain monodispersed emulsions, choosing a uniform membrane is not sufficient (14). In premix ME a narrower PSD was obtained using SPG than PTFE membranes (17).

The aim of this work is to show that monodispersed emulsions with a span of PSD of 0.42-0.56 measured by a light scattering particle size analyzer can be produced using α-Al_2O_3 membrane under the wide range of operating conditions. For the purpose of this work, emulsions will be regarded as monodispersed if the PSD span is smaller than 0.6. In all previous studies dealing with α-Al_2O_3 or Zr_2O_3 ME (18-21), the reported spans of PSD were about 0.83 (18) and in some cases above 0.87 (19). We have conducted many experiments resulting in the span of PSD of less than 0.5, which is some 40 % less than the smallest span reported till now. One of the possible explanations is a relatively large mean pore size of 1.4 μm used in our experiments, while in previous investigations the mean pore size was mainly 0.1-0.5 μm. According to our SPG emulsification results (6), a larger mean pore size often yields a smaller span. However, we have also conducted an experiment with 0.5-μm α-Al_2O_3 membrane, which resulted in the span of PSD of 0.59. We believe that it was due to careful membrane cleaning by ultrasonication after each experimental series. One of the objectives of this work is to investigate the range of operating parameters under which such a narrow PSD can be obtained.

EXPERIMENTAL

Materials

Emulsions were prepared using rapeseed oil (Floreal GmbH, Germany) as the dispersed phase and 2 wt. % Tween 80 (polyoxyethylene (20) sorbitan monooleate, Merck GmbH, Germany) dissolved in demineralized water as the continuous phase. The vegetable oil was treated before usage with 60 g l^{-1} silica gel (Silica gel 60, Merck GmbH) to remove

impurities which could cause membrane fouling. This treatment involved the adsorption of impurities on silica particles in a stirring vessel for 24 h, followed by centrifugation at 9000 rpm for 2 × 30 min. The physical properties of both phases at 298 K determined using a Carri-Med model CSL-100 controlled stress rheometer and a Prolabo model T.D. 2000 tensiometer-densimeter are given in Table 1.

Membranes and Membrane Module

Ceramic α-Al_2O_3 membranes (250 mm length × 7 mm inner diameter) were supplied from Membraflow GmbH & Co. KG (Aalen, Germany) with a mean pore size of 1.4 and 0.5 μm. These membranes are composed of a skin layer with the thickness of 20-30 μm and porosity of 0.35, supported by a 2-mm thick porous substructure. The effective membrane area in the module was 50.0 cm^2.

Experimental Set-up and Procedure

Emulsions were prepared using a cross-flow ME system described elsewhere (6). The continuous phase/emulsion was recirculated inside the membrane tube using a Netzsch model NL 20 Mohno-pump (Waldkraiburg, Germany). This pump is a low shear type and causes no droplet break-up while the emulsion is recirculating through the equipment. The oil phase was placed in a pressure vessel and introduced at the annular space of the module with compressed air. The weight of oil phase permeated through the membrane was measured by a balance on which the pressure vessel rested. The balance was interfaced to a PC computer to continuously collect time and mass data.

The experiments have been carried out over a wide range of shear stress at the membrane wall of 0.55-139 Pa, which corresponded to crossflow velocity of the continuous phase in the membrane tube of 0.34-6.9 m/s and tube Reynolds number of 1,700-34,000 (Fig. 2). The wall shear stress was calculated using the expression:

$$\sigma_w = (d_i / 4)(\Delta p_{fr} / L) \qquad (1)$$

where d_i is the inner diameter of the membrane tube and Δp_{fr} is the pressure drop for overcoming friction resistance in the membrane tube over a length L. In the special case of laminar flow inside the membrane tube ($Re_t < 2300$), Eq. (1) is simplified to: $\sigma_w = 8\mu_c v_t/d_i$, where v_t is the mean velocity of continuous phase inside the membrane tube and μ_c is the continuous phase viscosity given in Table 1. In the case of turbulent flow, Eq. (1) has the following form:

$$\sigma_w = \lambda(\rho_c v_t^2 / 8)$$

where ρ_c is the continuous phase density (Table 1) and λ is the Moody friction factor, which is at $2{,}500 < Re_t < 100{,}000$ given by the well-known Blasius equation:

$$\lambda = 0.3164\,Re_t^{-0.25}$$

Transmembrane pressure was in the range of 52-170 kPa, which was 2.3-7.4 times greater than the capillary (Laplace) presssure. The transmembrane pressure was calculated as a difference between the dispersed phase pressure and the mean pressure of continuous phase. In most experiments, the mean pore size was 1.4 μm and the final dispersed phase (oil) content was 1 vol. %.

After each experimental series, the whole crossflow system was cleaned in place with 1 wt. % cleaning agent P3-ultrasil 53 (Henkel KGaA) at 323 K for 1 h. However, cleaning in place (CIP) was not enough to restore the initial membrane permeability. Therefore, the module was dismantled and the membrane was additionally cleaned in an ultrasonic bath at 343 K for at least several hours using a commercial detergent solution. The detergent solution was then removed from the membrane pores by ultrasonication with demineralized water.

Determination of Mean Droplet Size and Particle Size Distribution (PSD)

Particle size distribution was measured by a Coulter LS 230 light scattering particle size analyser using Polarization Intensity Differential Scattering (PIDS) technology, which allowed the measurement of particles in the size range of 0.04-2000 μm using 116 size channels. The mean droplet size was expressed as the Sauter mean diameter, $d_{3,2}$, which is the diameter of a spherical particle having the same area per unit volume as that of the total collection of particles in the emulsion (22).

RESULTS AND DISCUSSION

Rate of Oil Permeation through the Membrane

The typical oil mass vs. time data collected during the experiments are shown in Fig. 3. Except at 60 kPa, the time interval of 8-40 min was enough to reach the oil content in emulsion of 1 vol. %. Virtually no changes in the permeation rate with time were observed, since the experiments were short. In a much longer experiment, in which the oil content in emulsion of 20 vol. % was reached, the oil flux increased with time, as found in earlier investigations (19, 20). As expected, the rate of oil permeation increased with transmembrane pressure.

Oil fluxes, J_d, were calculated from the slope of the mass vs. time lines and shown in Fig. 4 as a function of transmembrane pressure, Δp_{tm}. The slope of J_d vs. Δp_{tm} lines increased with Δp_{tm} for each σ_w value, indicating that the proportion of simultaneously active pores increased with increasing the transmembrane pressure. The capillary pressure of p_{cap} = 23 kPa was estimated by extrapolating the J_d vs. Δp_{tm} lines to $J_d = 0$. According to the Laplace equation:

$$p_{cap} = \frac{4\gamma_\infty \cos\theta}{d_p}$$

where $\gamma_\infty = 8 \times 10^{-3}$ N/m is the equilibrium interfacial tension between the continuous and dispersed phase, $d_p = 1.4 \times 10^{-6}$ m is the mean pore size of the membrane and θ is the contact angle between the dispersed phase and membrane surface. Assuming that

the membrane surface was totally wetted with the continuous phase ($\theta = 0$), one obtains p_{cap} = 23 kPa, which is equal to the experimentally found p_{cap} value. The dispersed phase flux increased with increasing the wall shear stress, which was found earlier for a 0.8-μm α-alumina membrane (20).

Influence of Process Parameters on the Mean Droplet Size and PSD

Influence of transmembrane pressure

As shown in Fig. 5, the mean droplet size diminished initially with the transmembrane pressure, and then increased with continued increase in Δp_{tm}. The initial decrease in mean droplet size by 0.9-1.2 % can be explained by the assumption that in the vicinity of capillary pressure only the largest pores are active. Therefore, the mean droplet size is then larger than at the higher pressures, at which the smaller pores also take part in droplet formation. Transmembrane pressure at which the mean droplet size was minimal was the optimum transmembrane pressure with regard to droplet size uniformity. In our experiments this optimum pressure increased with the wall shear stress and it was 60-80 kPa, i.e. the optimum $\Delta p_{tm}/p_{cap}$ ratio was 2.6-3.5. The wall shear stress of 0.55 Pa was too small for the droplets to detach fast enough at $\Delta p_{tm} > 90$ kPa and as a result, a strong increase of the mean particle size due to uncontrollable droplet grow and coalescence at the membrane surface was observed under these conditions. At the wall shear stress of 47-139 Pa, the increase in $d_{3,2}$ with increasing Δp_{tm} above the optimum level was much less pronounced. The increase in mean droplet size with transmembrane pressure was also found by other authors (23, 20).

Fig. 6 shows that with increasing the transmembrane pressure, the PSD curve becomes broader and broader. At a very high wall shear stress of σ_w = 139 Pa the emulsion was monodispersed at $\Delta p_{tm} \leq 170$ kPa corresponding to $J_d \leq 43.8$ l m^2 h^{-1}. As Δp_{tm} increases, the membrane productivity increases but the droplet size uniformity decreases, which means that in practical applications a balance must be found between these two opposing requirements.

Influence of wall shear stress

The mean droplet size decreased exponentially with increasing the wall shear stress, as shown in Fig. 7. At higher wall shear stress the droplets are sooner detached from the pore openings and the average distance between two neighbouring droplets increases. Therefore, the likelihood of droplet-droplet interactions at the membrane surface decreases and both smaller and more uniform droplets are formed. At the high transmembrane pressure of 120-140 kPa, the mean droplet size decreased sharply as σ_w increased from 0.6 to 47 Pa and then it became more or less independent of σ_w. At smaller transmembrane pressures the decrease in $d_{3,2}$ with σ_w was less pronounced. Scherze et al. (23), using microporous glass membranes (MPG) with d_p = 0.2-0.5 μm and milk proteins as emulsifiers, found that as σ_w exceeded 10 Pa the mean droplet size was only slightly influenced. Joscelyne and Trägårdh (19), using α-alumina and zirconia membranes with d_p = 0.2-0.5 μm for the preparation of mothers' milk replacement model emulsions, observed a strong affect of σ_w on the mean droplet size at $\sigma_w < 30$ Pa, which is similar to our results. However, Katoh et al. (24), using a MPG

membrane with d_p = 0.57 μm to prepare food emulsions, found that when $\sigma_w \geq 0.5$ Pa the mean droplet size was independent on the wall shear stress.

As shown in Fig. 8, the span of PSD at the optimum pressure difference of 60-70 kPa ranged from 0.48 to 0.42 and decreased as σ_w increased. As a comparison, Williams at al. (18) obtained a span of PSD of 0.82 at σ_w = 6 Pa and J_d = 8 l m^{-2} h^{-1} using α-alumina membranes with d_p = 0.2-0.5 μm. At low wall shear stresses and high transmembrane pressures (e.g., the dotted line in Fig. 8) the droplets grow and coalesce at the membrane surface before finally being carried away.

Influence of dispersed phase content, i.e. emulsification time

The influence of dispersed phase content on PSD during a single experiment at σ_w = 68 Pa and Δp_{tm} = 100 kPa is shown in Fig. 9. Here, it was more convenient to plot the particle size in a logarithmic axis, while the total range of particle sizes was more than one order of magnitude. It can be seen that the mean droplet size (3.79 ± 0.06 μm) and the span (0.51 ± 0.01) were remarkably constant up to 10 vol. %, i.e. for about 5 hours of operation. However, as dispersed phase content increased from 10 to 15 vol. %, the mean droplet size and the span increased due to the occurance of larger droplets in emulsion. It can be attributed to the wetting of membrane pores with the oil phase but the additional experiments are needed to confirm this statement. Using α-Al_2O_3 and MPG membranes, some authors reported that mean droplet size and span were nearly constant up to a dispersed phase content of 20-25 vol. % (18, 24).

Comparison with SPG Membranes, and the Results of Other Authors

The O/W emulsions prepared with Shirasu porous glass (SPG) and α-alumina membranes under the same operating conditions and using the same emulsion formulation were compared in Fig. 10. It can be seen that for the same pore size the better droplet size uniformity was achieved using SPG membranes (the span of PSD was 0.3-0.45 for SPG emulsification and 0.51-0.59 for α-alumina membranes).

In Fig. 11, a typical PSD curve in this work is compared with the PSD curves obtained by Schröder (20, 21, 25) using the same 1.4-μm α-alumina membrane. In this work, the membrane was cleaned by the CIP method followed by cleaning in an ultrasonic bath, while in the Schröder's experiments only the CIP method was used. In the latter case the broader PSD curves were obtained, especially if Tween 20 was used as emulsifier, since it adsorbs at newly formed water-oil interfaces much slower than SDS (21).

CONCLUSIONS

Monodispersed O/W emulsions with a span value of 0.42-0.56 were prepared using a 1.4-μm α-alumina membrane over a wide range of transmembrane pressures and wall shear stresses. The mean droplet size decreased initially with the transmembrane pressure, due to gradual activation of smaller pores, and then increased with the further pressure increase. The smallest mean droplet sizes and span values were obtained at the highest wall shear stress of 139 Pa. A narrow particle size distribution with the span of 0.48-0.49 was even obtained at the wall shear stress of 0.55 Pa, provided that $\Delta p_{tm}/p_{cap} \leq$

3.9. In order to control droplet size at $\Delta p_{tm}/p_{cap} \geq 5.2$, a wall shear stress of at least 47 Pa was necessary. Using the same emulsion formulation, the α-alumina membranes gave a broader PSD than Shirasu porous glass (SPG) membranes.

LIST OF SYMBOLS

d	particle diameter, m
d_i	inner diameter of membrane tube, m
d_p	mean pore size of membrane, m
$d_{3,2}$	Sauter mean diameter, m
J_d	dispersed phase flux, m s^{-1}
L	length of membrane tube, m
p_{cap}	capillary pressure, Pa
Δp_{tm}	transmembrane pressure, Pa
Δp_{fr}	pressure drop for overcoming friction resistance in membrane tube, Pa
Re_t	Reynolds number in membrane tube
t	time, s
v_t	mean velocity of continuous phase in membrane tube, m s^{-1}
μ_c	viscosity of continuous phase, Pa·s
ρ_c	density of continuous phase, kg m^{-3}
σ_w	shear stress in continuous phase at membrane surface (wall shear stress), Pa
φ	volume proportion of dispersed phase in emulsion, vol. %
γ_∞	equilibrium interfacial tension between dispersed and continuous phase, N m^{-1}

θ contact angle between dispersed phase and membrane surface wetted with continuous phase, rad

ACKNOWLEDGEMENT

The authors wish to thank the Alexander von Humboldt Foundation, Bonn, Germany for the financial support of this work.

REFERENCES

1. Nakashima, T.; Shimizu, M.; Kukizaki, T. Membrane Emulsification, Operation Manual, 1st Ed.; Industrial Research Institute of Miyazaki Prefecture: Miyazaki, Japan, 1991.

2. Joscelyne, S.M.; Trägårdh, G. Membrane emulsification – a literature review. J. Membr. Sci. **2000**, 169, 107-117.

3. Nakashima, T.; Shimizu, M. Porous glass from calcium alumino boro-silicate glass. Ceramics Japan **1986**, *21* (5), 408-412.

4. Nakashima, T.; Shimizu, M.; Kukizaki, M. Effect of surfactant on production of monodispersed O/W emulsion in membrane emulsification. Kagaku Kogaku Ronbunshu **1993**, *19* (6), 991-997.

5. Shimizu, M.; Nakashima, T.; Kukizaki, M. Preparation of W/O emulsion by membrane emulsification and optimum conditions for its monodispersion. Kagaku Kogaku Ronbunshu **2002**, *28* (3), 310-316.

6. Vladisavljević, G.T.; Schubert, H. Preparation and analysis of oil-in-water emulsions with a narrow droplet size distribution using Shirasu-porous-glass (SPG) membranes. Desalination **2002**, *144* (1-3), 167-172.

7. Shimizu, M.; Nakashima, T.; Kukizaki, M. Particle size control of W/O emulsion by means of osmotic pressure as driving force. Kagaku Kogaku Ronbunshu **2002**, *28* (3), 304-309.

8. Vladisavljević, G.T.; Lambrich, U.; Nakajima, M.; Schubert, H. Production of O/W emulsions using SPG membranes, ceramic α-Al_2O_3 membranes, microfluidizer and a microchannel plate – a comparative study. Proceedings of the 38th International SPG Forum, Miyazaki, Japan, Nov 21-22, 2002; The Society of SPG Technology: Miyazaki, 2002; 59-62.

9. Vladisavljević, G.T.; Schubert, H. Production of emulsions with a narrow droplet size distribution using a crossflow Shirasu porous glass (SPG) membrane. Abstracts, The 3rd World Congress on Emulsion, Lyon, France, Sept 24-27, 2002; 225.

10. Yasuno, M.; Nakajima, M.; Iwamoto, S; Maruyama, T.; Sugiura, S.; Kobayashi, I.; Shono, A.; Satoh, K. Visualization and characterization of SPG membrane emulsification. J. Membr. Sci. **2002**, *210* (1), 29-37.

11. Suzuki, K; Shuto, I.; Hagura, Y. Characteristics of the membrane emulsification method combined with preliminary emulsification for preparing corn oil-in-water emulsions. Food. Sci. Technol. Int. **1996**, *2* (1), 43-47.

12. Kukizaki, M.; Nakashima T.; Shimizu, M. Preparation of new asymmetric type of porous glass and effect of its structure on microfiltration. Membrane **2002**, *27* (6), 324-330.

13. Nakashima, T; Shimizu M.; Kukizaki, M. Particle control of emulsion by membrane emulsification and its applications. Adv. Drug Deliv. Rev. **2000**, *45*, 47-56.

14. Abrahamse, A.J.; van Lierop, R.; van der Sman, R.G.M.; van der Padt, A.; Boom, R.M. Analysis of droplet formation and interactions during cross-flow membrane emulsification. J. Membr. Sci. **2002**, *204*, 125-137.

15. Vladisavljević, G.T.; Tesch, S.; Schubert, H. Preparation of water-in-oil emulsions using microporous polypropylene hollow fibers: Influence of some operating parameters on droplet size distribution. Chem. Eng. Process. **2002**, *41* (3), 231-238.

16. Kobayashi, I.; Yasuno, M.; Iwamoto, S.; Shono, A.; Satoh, K.; Nakajima, M. Microscopic observation of emulsion droplet formation from a polycarbonate membrane. Colloid. Surface. A **2002**, *207* (1-3), 185-196.

17. Suzuki, K.; Fujiki, I.; Hagura, Y. Preparation of high concentration of O/W and W/O emulsions by the membrane phase inversion emulsification using PTFE membranes. Food Sci. Technol. Int. Tokyo **1999**, *5* (2), 234-238.

18. Williams, R.A.; Peng, S.J.; Wheeler, D.A.; Morley, N.C.; Taylor, D.; Whalley, M.; Houldsworth, D.W. Controlled production of emulsions using a crossflow membrane. Chem. Eng. Res. Des. **1998**, *76A* (19), 902-910.

19. Joscelyne, S.M.; Trägårdh, G. Food emulsions using membrane emulsification: conditions for producing small droplets. J. Food Eng. **1999**, *39*, 59-64.

20. Schröder, V.; Schubert, H. Production of emulsions using microporous, ceramic membranes, Colloid. Surface. A **1999**, *152*, 103-109.

21. Schröder, V.; Behrend, O.; Schubert, H. Effect of dynamic interfacial tension on the emulsification process using microporous, ceramic membrane. J. Colloid Interface Sci. **1999**, *202*, 334-340.

22. Coulson, J.M.; Richardson, J.F. Particulate Solids. In *Chemical Engineering*; 3rd Edition; Pergamon Press: Oxford, 1985; Vol. 2, 10.

23. Scherze, I.; Marzilger, K.; Muschiolik, G. Emulsification using micro porous glass (MPG): surface behaviour of milk proteins. Colloids and Surfaces B **1999**, *12*, 213-221.

24. Katoh, R.; Asano, Y.; Furuya, A.; Sotoyama, K.; Tomita, M. Preparation of food emulsions using a membrane emulsification system. J. Membr. Sci. **1996**, *113*, 131-135.

25. Schröder, V. Herstellen von Öl-in-Wasser-Emulsionen mit mikroporösen Membranen. Ph.D. thesis; University of Karlsruhe (T.H.): Karlsruhe, Germany, 1999.

TABLES

Table 1. The density and viscosity of the dispersed and continuous phase used in this work

	ρ / kg m^{-3}	μ / mPa·s
Dispersed phase	920	58
Continuous phase	1005	1.42

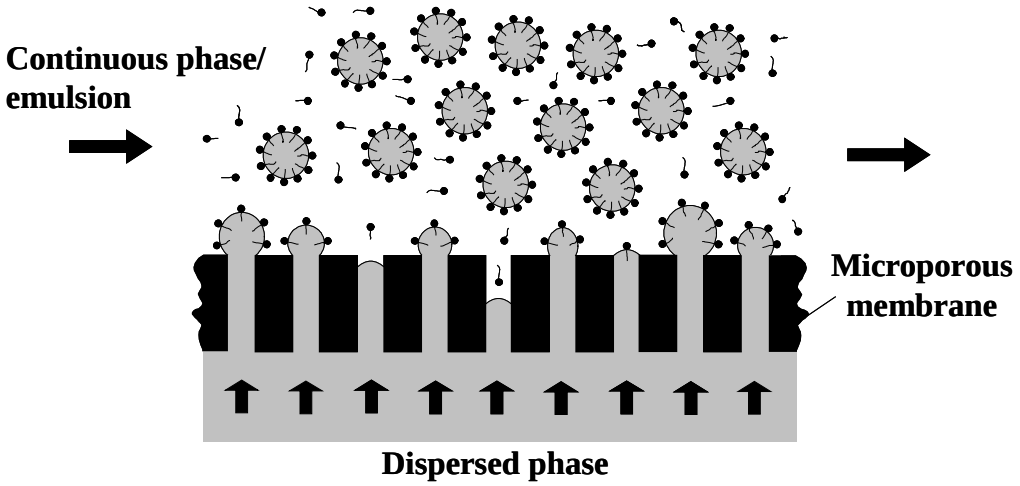

Figure 1. Schematic diagram of crossflow membrane emulsification.

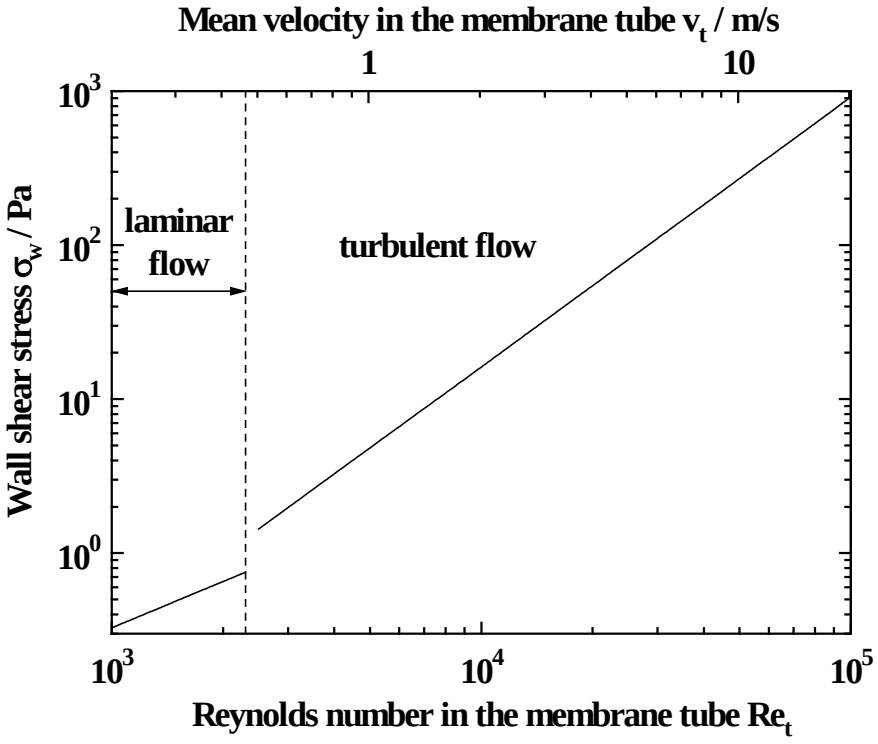

Figure 2. The variation of wall shear stress in our experiments with the Reynolds number and mean velocity of continuous phase in the membrane tube.

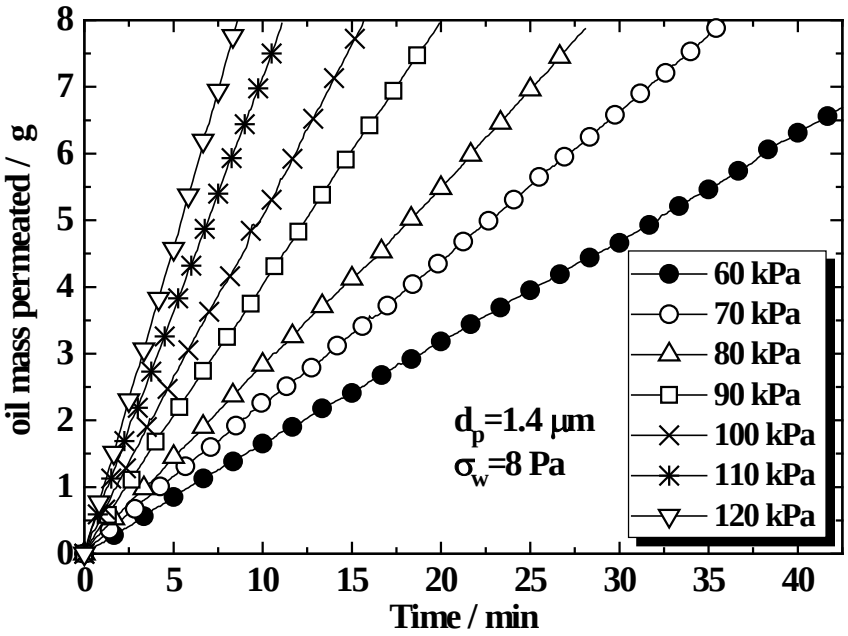

Figure 3. Typical permeation oil mass vs. time curves (φ_{max} = 1 vol. %).

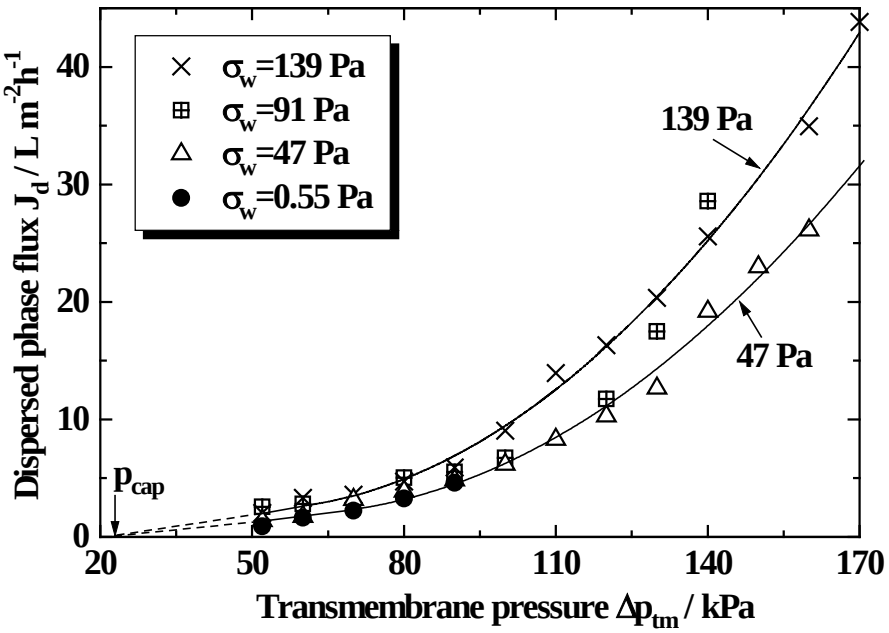

Figure 4. Influence of transmembrane pressure on the dispersed phase flux at different wall shear stresses.

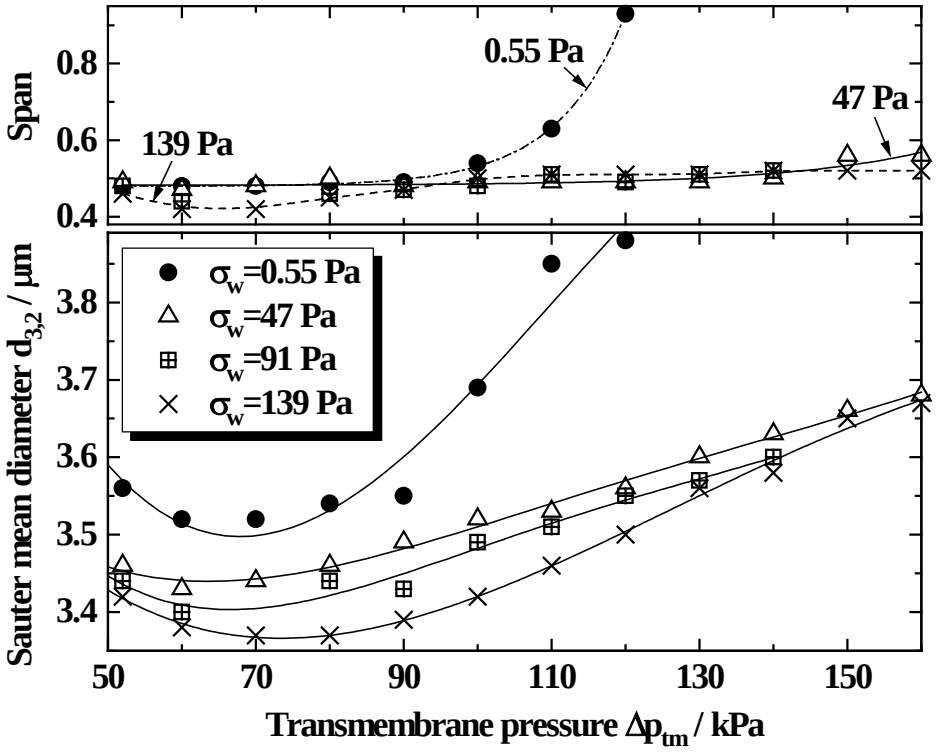

Figure 5. Influence of transmembrane pressure on the mean droplet size and the span of PSD at different wall shear stresses.

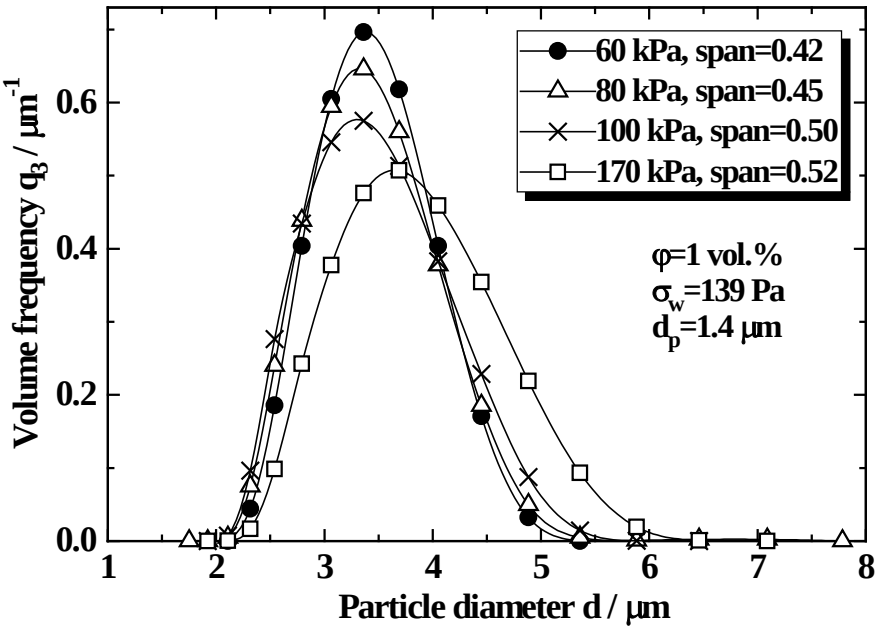

Figure 6. Influence of transmembrane pressure on the PSD.

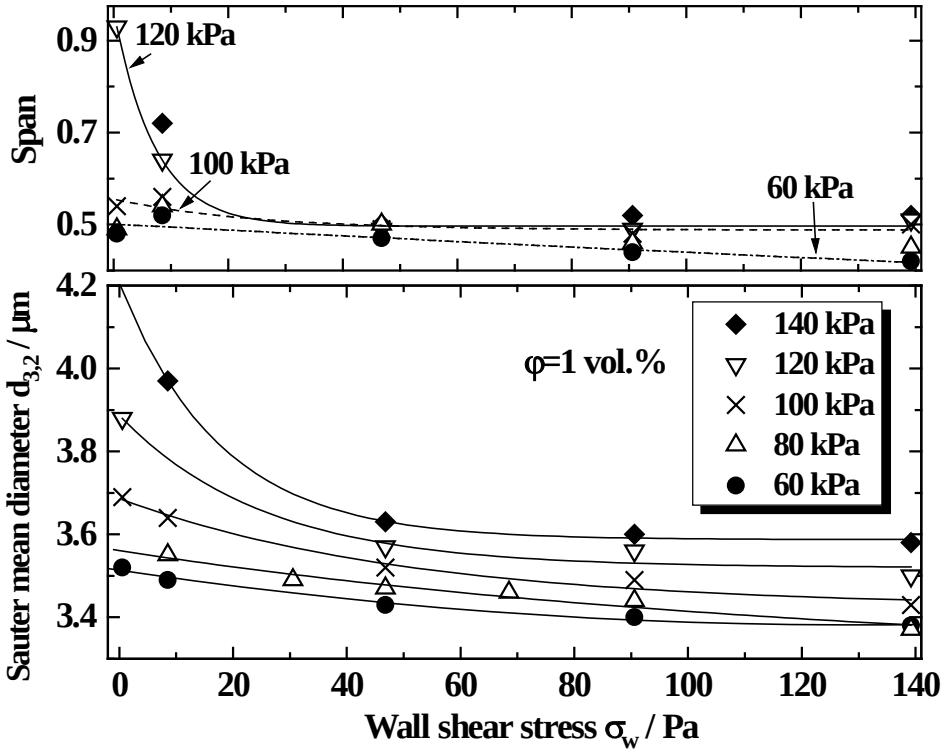

Figure 7. Influence of wall shear stress on the mean droplet size and the span of PSD at different transmembrane pressures.

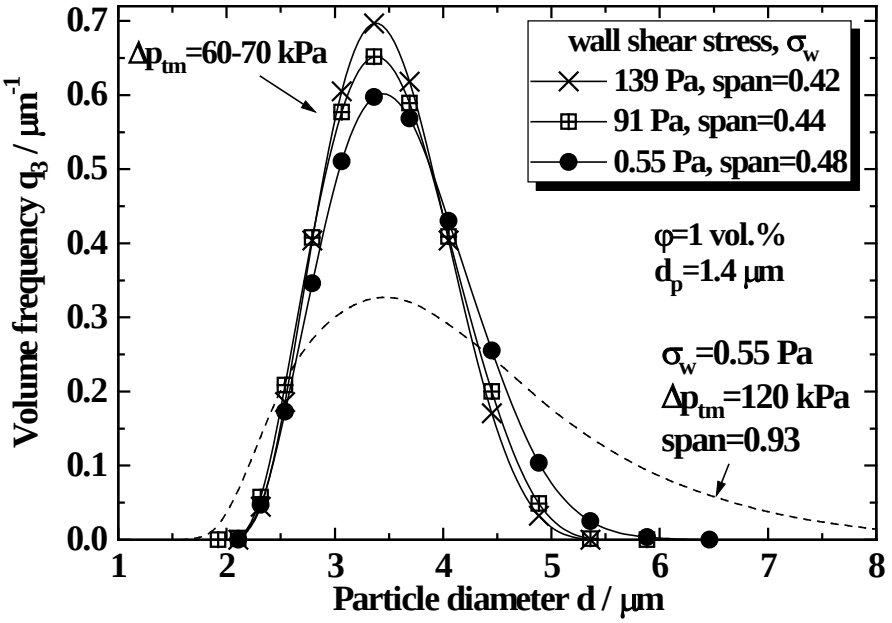

Figure 8. Influence of wall shear stress on the PSD.

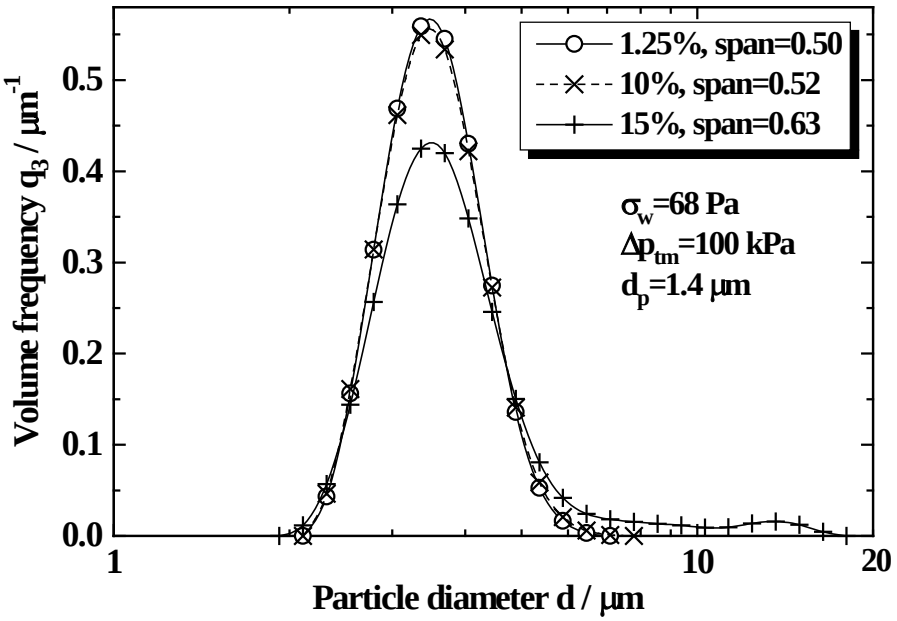

Figure 9. Influence of dispersed phase content, i.e. emulsification time on the PSD.

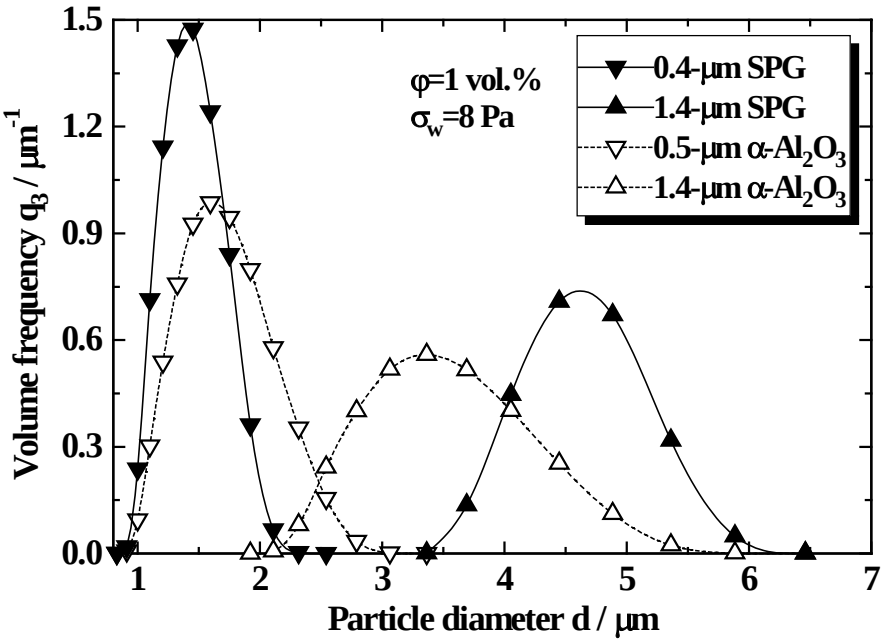

Figure 10. Influence of membrane structure (SPG and α-alumina) on the PSD.

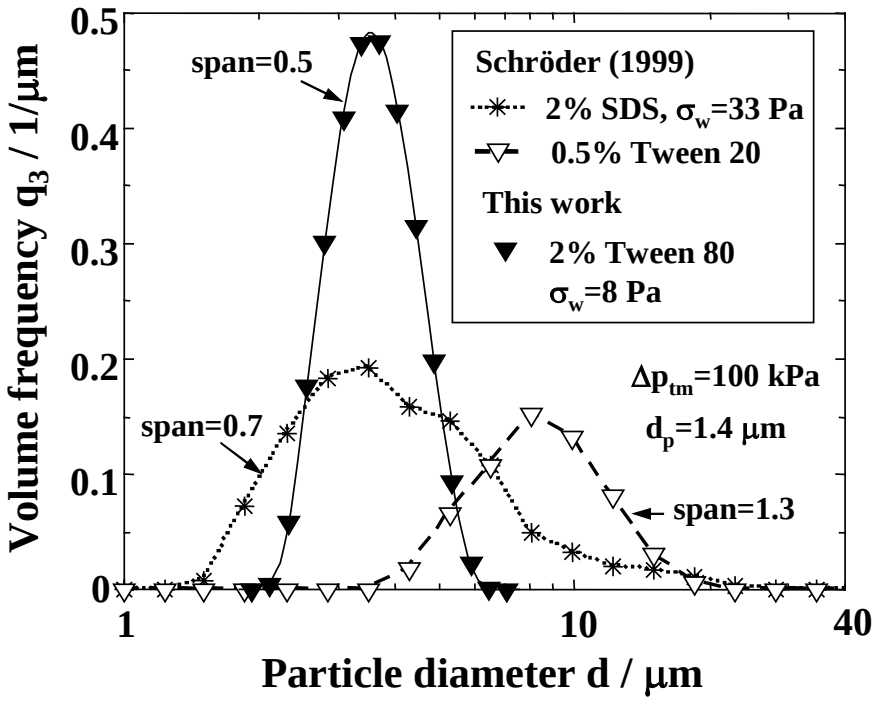

Fig 11. Comparison of PSDs obtained in this work with those reported by Schröder (25).